JOURNAL OF IMAGING SCIENCE AND TECHNOLOGY • Volume 40, Number 5, Sept./Oct. 1996

New Aspects for the Description of Liquid Immersion Development

G. Bartscher* and J. Breithaupt

Technical Electronics Institute, Aachen University of Technology, 52056 Aachen, Germany

The process of liquid immersion development (LID) has been thoroughly investigated theoretically and experimentally. Special interest has been devoted to the influence of space charge. The study reveals that the linear model commonly used for the description of the development process is not valid for typical conditions of LID. Consequently a model is proposed that considers such complexities as space charges and, in a first approximation, charge generation and turbulences. Special methods presented for measuring the parameters describing the toner suspension for LID minimize the influence of the stated complexities. With these parameters, our model achieves a better accuracy over a wide range of toner concentrations and electric field strengths than other known models for the LID process. We believe that coupling between space charge and turbulence effects for high concentrations leads to a considerably more accelerated development than that predicted by a linear or space-charge model. Additionally, the coupling leads to an approximately linear relationship as long as development does not come to saturation.

The Journal of Imaging Science and Technology 40: 441–452 (1996)

Introduction

Since the invention of liquid toners in 1955 by Metcalfe,[1] the method of liquid immersion development (LID) for developing electrostatic images has established itself as an alternative to dry toning. The main advantage of LID is the small diameter of the dye particles in the liquid toner of typically 1 µm compared with 8 µm for dry toners. The finer particles lead to higher spatial resolution and better gray-scale capabilities.

For a specific system (e.g., a printer using LID) it is of great interest to be able to calculate the amount of deposited toner, and thus the gray scale of the developed image, as a function of the electric field (caused, for example, by the surface charge on a photoconductor) and the properties characterizing the liquid developer. Numerous papers dealing with this problem,[2–13] as well as the determination of the properties of the liquid developer, have been published.[3–15] Despite this considerable effort many problems are not yet understood in detail.

Our interest in LID comes from a new printing technology, which we call ELPHI.[16,17] This process uses an electronic print plate with a controllable electrode for every single pixel of the printed image and liquid toner. The gray scale of each pixel is changed by varying the development time. Consequently a better understanding of LID helps to achieve a more precise control of development and thus enhances the quality of the printed image. With this study we aim at a more complete understanding of LID. One of the main issues here is the effect of space charges.

The first part of the study deals with the theory of the LID process. After a description of the commonly used linear model, the influence of space charge is discussed. We derive circumstances under which space-charge effects may be neglected. For the description of LID with the consideration of space charges, a numeric algorithm is presented. In addition, other complexities such as charge generation and turbulences are discussed. First-order models for the description of these effects for LID are proposed and introduced into the SimLID computer program.

In the second part of this study, methods are presented that allow the determination of parameters that describe the liquid developer. Care has been taken to ensure that the above-mentioned complexities have minimal influence on the measurements.

The third and final part deals with a comparison of theoretically computed and experimentally measured data, including a discussion of the results.

LID Developers

During liquid immersion development, electrically charged particles in a liquid migrate under the influence of an electric field. This migration causes the deposition of charged dye particles (toner particles), so that, for example, a latent electrostatic image becomes visible. The liquid (that is, the LID developer, often just called *toner*) consists of three main ingredients and optionally several other additives. The three basic materials are an insulating carrier fluid, toner particles (consisting of pigment and resin), and a charge control agent (CCA). Even though most materials acquire an electrical charge when dispersed in an insulating fluid,[18] a more definite charge for the toner particles can be obtained by charge control agents such as carboxylic salts.[15] In the insulating fluid these additives form, e.g., inverse micelles, of which a small number acquire an electrical charge. Through charge exchange or other mechanisms a specific charge for the toner particles is obtained. Other additives may be present for enhanced colloidal stability and better fixation of the toner particles on paper after development.

This description leads to the following simplified model for the parameters characterizing the LID developer.[6,10] Three different types of charged particles are present: toner particles, excess ions, and counter ions. Excess and counter ions are the charged particles of the CCA. Excess ions have a charge of the same sign as the charge of the toner particles. Counter ions have a charge of opposite sign. Overall the liquid toner remains electrically neutral.

Each of the three particle types may be characterized by three values: the number of particles per volume n, the

---

Original manuscript received March 21, 1996.

* IS&T Member

electrical charge (absolute value) of each particle q, and the electrophoretic mobility μ. With these quantities the overall electrical neutrality of the LID developer may be written as

$$n^{(T)}q^{(T)} + n^{(X)}q^{(X)} = n^{(C)}q^{(C)}, \qquad (1)$$

with T for toner particles, X for excess ions, and C for counter ions. The electrical conductivity σ of the toner is given by the sum of the conductivities of the three particle species (the conductivity of the insulating carrier fluid can be neglected):

$$\sigma = n^{(T)}q^{(T)}\mu^{(T)} + n^{(X)}q^{(X)}\mu^{(X)} + n^{(C)}q^{(C)}\mu^{(C)}. \qquad (2)$$

This model is the basis for the various models for the description of the LID process.

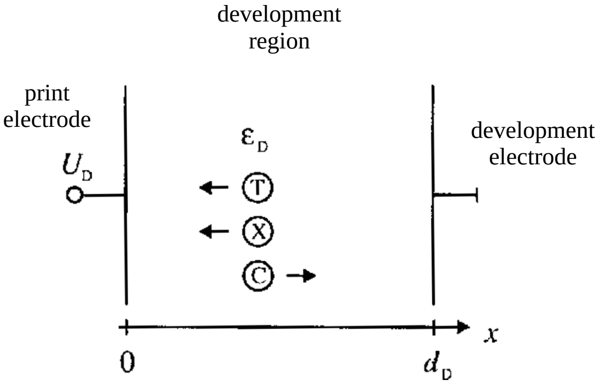

Figure 1. Model for the process of LID between two metal electrodes. Three types of charged particles are considered, namely, toner particles (T), excess ions (X), and counter ions (C).

Theory for the Linear Model

The most common application for LID is the printing of images, so any theory for liquid immersion development has to describe the amount of deposited toner particles as a function of external parameters (e.g., the applied voltage) and internal parameters (e.g., n, q, μ).

Our first model for LID (referred to as the "linear model") is basically identical to a commonly used model originally introduced by Stark and Menchel[4] and Kurita.[19] Our calculations are further simplified due to the absence of a photoconductor. This and the corresponding models from other authors are applicable only to broad area development. Throughout this study we discuss only models in which spatial changes are only considered in the x direction, while changes in y and z directions are neglected.

Figure 1 illustrates a configuration for the development of toner particles between two metal electrodes separated by the distance d_D and filled with a liquid with a dielectric constant of ε_D. The applied voltage U_D causes an electric field in the development region E_D given by the simple relation:

$$E_D = \frac{U_D}{d_D}. \qquad (3)$$

This electric field causes a migration of the charged particles as indicated in Fig. 1. If no space charge and no surface charge are considered, E_D does not change with time. Thus, for a calculation of the number of toner particles per unit area $N^{(T)}(t)$ deposited on the print electrode as a function of time, we need only know the number of toner particles per volume, $n^{(T)}$, and the mobility of the toner particles, $\mu^{(T)}$:

$$N^{(T)}(t) = n^{(T)}\mu^{(T)}\frac{U_D}{d_D}t. \qquad (4)$$

With $N^{(T)}$, the deposited mass per unit area or the optical density can easily be derived if the density (mass per volume) and radius of toner particles is known.[20]

Validity Range of the Linear Model

We now consider the question under which Eq. 3 (and thus Eq. 4) is a good approximation. For a space-charge density $\rho(x)$ $(0 < x < d_D)$ in the development region, Eq. 3 must be extended to[21]

$$E_D = E_D(x) = E_D^{lin} + E_D^{\rho}(x), \qquad (5)$$

with E_D^{lin} as in Eq. 3 and E_D^{ρ} the additional field created by space charges:

$$E_D^{\rho}(x) = \frac{1}{\varepsilon_D\varepsilon_0}\left[\int_0^x \rho(x')dx' - \frac{1}{d_D}S(d_D)\right], \qquad (6)$$

with an integral part

$$S(d_D) = \int_0^{d_D}\left[\int_0^{x'} \rho(x'')dx''\right]dx'. \qquad (7)$$

It is straight forward that Eq. 4 can be a good approximation for the development process only if

$$\left|E_D^{\rho}(x)\right| << \left|E_D^{lin}\right| \qquad (8)$$

is valid for all times t and all places x in the development region. To obtain an estimate of $\left|E_D^{\rho}(x)\right|$ we consider the case where the space-charge influence becomes most pronounced. This happens when all particles of one polarity have been swept out of the development region and only those of the opposite polarity are left. Assuming that the negative particles have been swept out prior to any movement of the positive particles, they cause a homogeneous charge density $\rho_0 > 0$. This leads to:

$$\left|E_D^{\rho}(x)\right| = \frac{\rho_0}{\varepsilon_D\varepsilon_0}\left|x - \frac{1}{2}d_D\right| \le \frac{\rho_0 d_D}{2\varepsilon_D\varepsilon_0}. \qquad (9)$$

With this relation Eq. 8 becomes:

$$\rho_0 << \frac{2\varepsilon_D\varepsilon_0|U_D|}{(d_D)^2}. \qquad (10)$$

As a typical example, an LID process is characterized by d_D = 1 mm, ε_D = 2, U_D = 500 V, and ρ_0 = 0.5 C/m^3, respectively. With these values the right-hand side of Eq. 10 is 0.018 C/m^3, so that the condition for negligible space charge is far from being valid.

Even though this calculation has been done for metal electrodes, it is also valid for a development process with a photoconductor, assuming that the thickness of the photoconductor is much smaller than the width of the development region d_D. Consequently, if space charges cannot be neglected, a theory of liquid immersion development must take this effect into account. Such a theory is presented in the following section. Similar models have already been reported by Crofoot and Cheng,[22] Chen,[23] and Davis and coworkers.[10] In addition to space charge, our model considers by an approximation charge generation and turbulence.

LID with Space Charge

So far, no analytical model for the description of liquid immersion development that takes space charges into account is known. Thus, a numerical algorithm is used. Whereas the models of the authors mentioned[10,22,23] numerically solve the nonlinear coupled partial differential equations, which result from the continuity equation and the calculation of the electric field similar to Eq. 5, we use an alternative algorithm that calculates the displacement of packages of charged particles (such algorithms are discussed in Ref. 24). This method has the advantage that it is nearer to the physical model, in which charged particles migrate under the influence of an electric field.

Our algorithm has three basic steps:

1. The electric field as a function of x is calculated considering applied voltage and space-charge distribution.
2. For packages of particles the displacement is calculated as a function of the local electric field. The field is held constant for the time Δt.
3. From the displacement of the packages a new space-charge distribution is calculated. Then the algorithm continues at the beginning.

In addition to the obvious division of the time t in intervals Δt, the development region is divided into intervals Δx. A PASCAL program implemented on a 486 personal computer has been written. It is called SimLID (*Sim*ulation of *L*iquid *I*mmersion *D*evelopment). SimLID has been thoroughly tested with several methods. For negligible space charges, analytical solutions such as Eq. 4 show excellent agreement with SimLID. Calculations with SimLID and parameters presented by Crofoot and Cheng[22] and Chen,[23] have been performed. Our results always show good qualitative, but in most cases poor quantitative, agreement with the mentioned papers. Deviations up to 50% occur.

To find a reason for these deviations, two additional methods for the verification of the SimLID results have been developed. First, another program, which directly solves the differential equations, was written, following the method of Crofoot and Chen. For sufficiently small values of Δx and Δt excellent agreement with SimLID is achieved. Secondly, an analytical solution for a special (though not observed in practice) case of liquid immersion development with only one type of charged particles was obtained.[25] Again excellent agreement with SimLID was found. Especially because of this verification method, we are confident that the results calculated by SimLID are correct.

The described algorithm has been extended, so that the simulation program SimLID is able to account for charge generation, as well as the toner flow due to pumping and diffusion effects. These parameters are discussed in the next section.

For the example of two types of particles with equal mobilities (excess ions are neglected here), Fig. 2 shows the results of SimLID. The number of deposited toner particles per unit area is plotted as a function of time t for different charge densities ρ_0. The positive toner particles have ρ_0 as an initial charge density, the negative counter ions $-\rho_0$. The number of deposited toner particles is normalized to the number of particles initially in the development region ($d_D n^{(T)}$). Other parameters are $d_D = 1$ mm, $\varepsilon_D = 2$, $U_D = 1000$V, and particle mobility $\mu = 10^{-9}$ m^2/Vs, respectively.

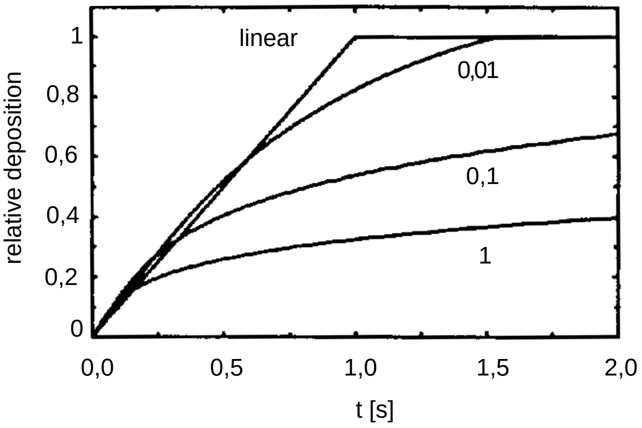

Figure 2. Example for the number of deposited toner particles on one electrode with and without (linear) the influence of space charge as a function of time. The parameter is the charge density ρ_0 (in units C/m^3).

In addition to $\rho_0 = 0.01$, 0.1, and 1 C/m^3 another curve is depicted. It is the curve for the linear model, which is calculated with a normalized form of Eq. 4. For the linear model, development ends when at $t = 1$ s all particles have been deposited. Generally, the consideration of space charge has two effects when compared with the linear model. The first effect is well known: Overall a higher charge density leads to slower development. The second effect is rather surprising: For a relatively short time development proceeds faster than with the linear model. Even though this effect has not been mentioned by previous authors,[10,22,23] a comparison of their data with the appropriate linear model reveals the same accelerating phenomenon.

An explanation for this effect can be found by looking at the transient behavior of the charged particles. Figure 3 shows the spatial distribution of the particles for different states together with the related electric field. Prior to the development process we have a situation as in Fig. 3(a). Figure 3(b) shows a hypothetical state for the charge distribution shortly after the beginning of the development. The electric field near the border of the development region is higher than the field of the initial state (dashed line). Thus particles move faster in these regions so that a higher deposition rate is observed. The state of Fig. 3(b) is not realistic, as a higher current density in the high-field regions will readily lead to a particle depletion. This is shown in Fig. 3(c) (a similar picture has been presented by Crofoot and Chen[22]). As a consequence, the accelerated development continues for only a limited period, after which the rate of development falls under the linear case. This is due to the space charges at the borders, which decrease the electric field in the center of the development region, so that a refilling of the depletion areas is rather slow.

Further Complexities

In addition to the discussed influence of space charge, several other influences complicate a theory for LID. Some of those thought to be most relevant are discussed briefly.

Charge Generation. Aside from the toner particles, a liquid toner contains a certain number of charged particles due to the CCA. Only a small amount of the mass of the CCA is actually charged (typically less than 1%).[10] If charged particles are removed from the liquid toner, e.g.,

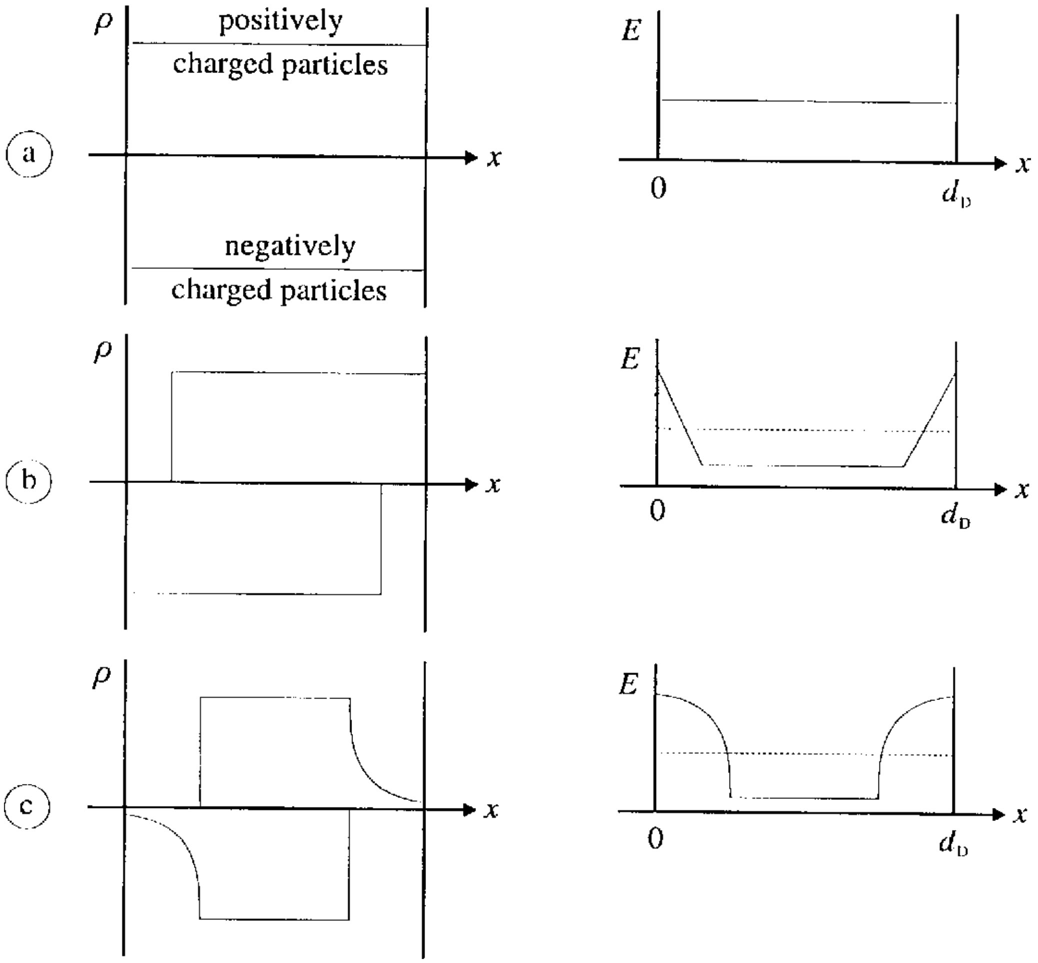

Figure 3. Different states of the LID process as a function of time for two types of particles (excess ions neglected). The left side shows the spatial distribution of the particles, the right side the related electric field. (a) is the situation of development for $t = 0$; (b) and (c) depict states for $t > 0$. A situation as shown in (b) is valid for negligible space charge, and (c) applies to strong space charge.

by an electric field, new charged particles are generated. The mechanism for the generation is, for example, a charge exchange between two formerly neutral inverse micelles. After the exchange, one micelle has a positive charge, the other a negative charge.

In first order, the generation process for one particle type can be described by

$$\frac{dn(t)}{dt} = g[n_0 - n(t)], \tag{11}$$

with $n(t)$ being the number of charged particles, n_0 the equilibrium value, and g the rate of generation for the charged particles. Of course, this generation does not apply for the toner particles. This description implies an infinite reservoir of uncharged CCA, which is a good approximation, as typically less than 1% of the mass of the CCA is charged. The simulation program SimLID takes into account generation effects within the limits of Eq. 11.

Laminar Toner Flow. In a typical LID device the liquid toner is actively pumped into the development region in order to minimize depletion. This typically laminar flow would not influence the development process if space charges were negligible, except that development would not be terminated after a certain time, as there is a continuous replacement of deposited particles. With space charge, interactions with toner flow are possible. A problem with the consideration of toner flow is that it actually implies a two-dimensional model, as the toner flow is perpendicular to the migration of the particles due to the electric field. For a first-order approximation, toner flow is described by a method similar to that used for charge generation. The only difference is that toner particles must also be considered here, and we thus have a “flow” constant f instead of a generation constant g. This constant f depends on the speed of the flow and on the length of the development region in the direction of the flow.

Diffusion. If a local change of the particle concentration occurs, a diffusion current $\tilde{j}$ proportional to the diffusion constant $\tilde{D}$ and the spatial concentration difference dn/dx results:

$$\tilde{j} = -\tilde{D}\frac{dn}{dx}. \tag{12}$$

The simulation program SimLID accounts for diffusion by interchanging particles of neighboring charge packages according to this relation.

Measurements of the diffusion constant for the CCA revealed $\tilde{D} = 10^{-9}$ m^2/s (±25%). Because of sedimentation effects, $\tilde{D}$ for the toner particles could not be measured. However, with a relation between $\tilde{D}$ and the electrophoretic mobility μ,[26]

$$\tilde{D} = \frac{\mu k_B T}{q}, \tag{13}$$

it can be shown that the diffusion constant for the toner particles is smaller than that for the CCA (Boltzmann constant, k_B; absolute temperature, T; particle charge, q). Simulations with SimLID for realistic conditions, as well as analytical calculations for idealized conditions, show that diffusion can normally be neglected. For a very long development time (approximately $t > 50$ s), diffusion is not negligible.

Turbulences. The existence of turbulences in the liquid toner during the development process has been reported by several authors.[6,7,27] Our own investigations with a transparent development cell show similar results. The expression *turbulences* includes all movements in the liquid that are not directly caused by the electric field or the mechanical pumping of the liquid. Because of the well-known complexity of the theory for such electrohydrodynamic turbulences, we have developed a rather simple semi-empirical method for a first-order approximation. The question is, in what way do turbulences affect the spatial particle distribution during development? Generally the rather chaotic movement caused by turbulences leads to an equalization of the particle distribution. Thus a first-order description can be achieved by simulating turbulences with a diffusion process. Consequently our approximation describes turbulences by a diffusion constant $\tilde{D}_{turb}$. Values for this constant $\tilde{D}_{turb}$ must be found empirically by fitting simulated and measured curves.

Distributions. Our theory, as well as all other known theories for LID, describes the parameters of the liquid toner by mean values. If, for example, the radius r of the toner particles is taken, it is clear that a certain distribution $p(r)$, rather than a single value r, is the appropriate description.[28] Because of the nonlinear dependence of the development process of such quantities as particle radius r or particle charge q, deviations will occur. Throughout this study such deviations are neglected and the given quantities typically represent the mean value of the associated distribution.

Measurement Methods for the Toner Parameters

Prior to any simulations for the comparison of simulated and measured data, the parameters characterizing the liquid developer must be determined. According to the section about LID developers, there are nine parameters: n, q, and μ for toner particles (T), excess ions (X), and counter ions (C). Additionally, radius and density (mass per volume) of the toner particles are required. With some reasonable assumptions the number of parameters is reduced to four.

For the calculations of time-dependent charge distribution and deposition, only the values of the initial charge densities ($\rho_0^{(T,X,C)} = n_0^{(T,X,C)} q^{(T,X,C)}$ are needed, not the separate values for the particle concentrations ($n_0^{(T,X,C)}$) and the particle charge ($q^{(T,X,C)}$). Excess and counter ions are assumed to be charged inverse micelles, so that their size and charge ought to be equal. Consequently we have equal mobilities for excess and counter ions:

$$\mu^{(X)} = \mu^{(C)} = \mu^{(XC)}. \tag{14}$$

Together with the condition for initial overall charge neutrality (Eq. 1), we now have four parameters left. For convenience we introduce the following quantities:

$$\rho_0 = \left|\rho_0^{(C)}\right| = \left|\rho_0^{(T)} + \rho_0^{(X)}\right|, \tag{15}$$

$$\varphi = \frac{\left|\rho_0^{(T)}\right|}{\rho_0}, \text{ and} \tag{16}$$

$$\lambda = \frac{\mu^{(XC)}}{\mu^{(T)}}. \tag{17}$$

Thus the four parameters for the description of the liquid toner are ρ_0 (charge density of all particles of one polarity), φ (ratio of the initial charge density of the toner particles to ρ_0), $\mu^{(T)}$ (electrophoretic mobility of the toner particles), and λ (ratio of the electrophoretic mobilities of excess and counter ions to toner particles). Later we show that for our measurements these four parameters are sufficient for a complete description of the toner.

Our methods for the determination of these parameters are based on ideas first published by Dahlquist and Brodie,[3] as well as Kohler and coworkers.[6] A similar method has recently been reported by Schein and coworkers.[13]

To explain our method we first calculate the current in the external circuit of a cell filled with liquid toner as a function of time. The situation is depicted in Fig. 1. Space charges are neglected, so that E_D is space and time independent. The current $I(t)$ caused by the toner particles, as well as excess and counter ions, is

$$I(t) = \frac{A\rho_0\mu^{(T)}U_D}{d_D}\left[\varphi\left(1-\frac{t}{\tau^{(T)}}\right)+(2-\varphi)\lambda\left(1-\frac{t}{\tau^{(XC)}}\right)\right], \tag{18}$$

where A is the area of the electrodes and

$$\tau^{(T)} = \frac{(d_D)^2}{\mu^{(T)}U_D}, \tag{19}$$

the time a toner particle needs to migrate through the development region. Accordingly, we have

$$\tau^{(XC)} = \frac{\tau^{(T)}}{\lambda}. \tag{20}$$

Note that the contribution of the excess and counter ions becomes zero for $t > \tau^{(XC)}$ and the contribution of the toner particles becomes zero for $t > \tau^{(T)}$. An example for $I(t)$ is shown in Fig. 4. Parameters here are $\lambda = 2$ and $\varphi = 0.8$.

Measurement of the current $I(t)$ under specific conditions results in a curve similar to Fig. 4. With the following relations the toner parameters can be extracted from the curve $I(t)$:

$$\mu^{(T)} = \frac{(d_D)^2}{\tau^{(T)}U_D}, \tag{21}$$

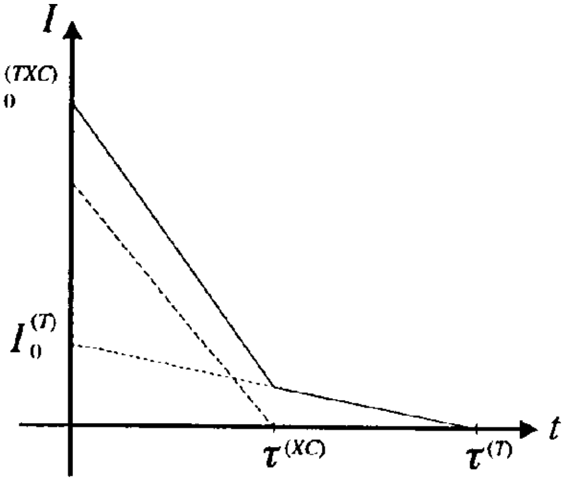

Figure 4. Calculated current in the external circuit of a cell filled with toner suspension. The total current (unbroken line) consists of two independent parts: a part due to the toner particles (finely dashed line) and a part due to the excess and counter ions (dashed line). For the depicted example, the parameters are $\varphi = 0.8$ and $\lambda = 2$.

$$\lambda = \frac{\tau^{(T)}}{\tau^{(XC)}}, \tag{22}$$

$$\rho_0 = \frac{d_D}{2\lambda A \mu^{(T)} U_D}\left(I_0^{(TXC)} + (\lambda - 1) I_0^{(T)}\right), \text{ and} \tag{23}$$

$$\varphi = \frac{2\lambda I_0^{(T)}}{I_0^{(TXC)} + (\lambda - 1) I_0^{(T)}}, \tag{24}$$

where $\tau^{(T)}$ is the time when the current $I(t)$ decreases to zero. It is assumed that the mobility of the toner particles is lower than the mobility of excess and counter ions, so that $\mu^{(T)}$ is related to $\tau^{(T)}$. This is verified experimentally, as explained later. The term $\tau^{(XC)}$ is the time when the rapidly decaying part of the current $I(t)$ decreases to zero. Finally $I_0^{(TXC)}$ is the measured current at $t = 0$, and $I_0^{(T)}$ is the current at $t = 0$ caused by the toner particles, which is determined by extrapolating the current for $t > \tau^{(XC)}$ back to $t = 0$.

Principally the described method is able to supply all four toner parameters. However, due to the discussed complexities, a realistic curve differs from the idealization of Fig. 4. By "realistic" we mean typical development conditions, as described in a previous section. Therefore conditions must be found such that the influence of the complexities is held as low as possible.

Space charges may be neglected when the condition of Eq. 10 is fulfilled. This condition is achieved by high voltages U_D, low distances d_D, and highly diluted toner suspensions leading to low ρ_0.

Turbulences arise from the interaction of the particles with the liquid. The electric field moves charged particles so that some irregular flow in the liquid is due to different mobilities. This flow, again, influences the movement of the particles. Roughly speaking the strength of the flow of the liquid depends on the mass of the initiating particles. Consequently, the low mass of a diluted toner suspension will cause less turbulence. This requirement corresponds to the condition for negligible space charge. However, the degree of dilution of the toner suspension is limited either by the sensitivity of the current measurement or by the inherent conductivity of the suspension fluid.

Finally, we must consider charge generation by the CCA. This effect has been shown to be not negligible for the investigated toner suspensions, and no way has been found to avoid it. Especially because of this effect, it has been difficult to determine $\tau^{(T)}$, and thus the mobility of the toner particles $\mu^{(T)}$, with the method described above. Therefore $\mu^{(T)}$ has been measured by the following method.

When space charges and other complexities can be neglected, the number of deposited toner particles per unit area $N^{(T)}$ is described by Eq. 4. In a relationship from Bayer,[29] $N^{(T)}$ is directly related to the optical transmission density D_{TR} through

$$D_{TR}(t) = A_0^{(T)} \lg(e) N^{(T)}(t), \tag{25}$$

with $A_0^{(T)}$ being the projected area of a toner particle and lg(e) the decadic logarithm of the base e of the natural logarithm. For spherical particles with radius $r^{(T)}$ we have $A_0^{(T)} = \pi\left[r^{(T)}\right]^2$.

To determine $\mu^{(T)}$ we now need values for $n_0^{(T)}$ and $r^{(T)}$. A value including both $n_0^{(T)}$ and $r^{(T)}$ can be readily obtained by measuring the optical transmission density of the toner fluid D_{FL}. For a layer of thickness d_{FL} we have

$$D_{FL} = A_0^{(T)} \lg(e) n_0^{(T)} d_{FL}. \tag{26}$$

With this relationship we finally achieve

$$D_{TR}(t) = \frac{D_{FL}}{d_{FL}} \mu^{(T)} \frac{U_D}{d_D} t. \tag{27}$$

Now we can determine $\mu^{(T)}$ by measuring the transmission optical density D_{TR} as a function of time t, because all other quantities in Eq. 27 are known. Because of the low optical density of the required diluted toners (e.g., D_{FL} = 0,02 for d_{FL} = 1 mm), these measurements are impracticable with a closed cell. Therefore, we used a cell in which continually fresh liquid flows through the development region, so that the achievable optical density is not limited by the amount of toner initially in the development region.

Experimental

We now briefly describe the equipment used for measurements. The goal of these measurements is twofold: first to determine the toner parameters for highly diluted suspensions, then, with these parameters, to compare simulated and measured data for higher toner concentrations. The black liquid toner used is a modification of a commercially available toner supplied by Olin Hunt (Belgium), called Toner J for our internal use. The original formulation is used for the electrofax process and is also well suited to electrographic recording. Toner J, which is obtained from the original by adding CCA, has been shown to give best results with the ELPHI process. A typical working solution contains 0.1% solids. Dilutions down to 0.001% have been used in order to minimize space charge and other disturbing effects.

Figure 5 shows the closed cell schematically. The lower electrode, which is made of aluminum, functions as the development electrode. The distance to the opposing (upper) electrode is defined by a Teflon spacer. Distances from 0.5 to 3 mm are used. A glass plate coated with ITO (indium tin oxide, an optically transparent and electrically conducting material) forms the upper electrode, so that for low dilution suspensions measurement of the transmission density caused by deposited particles is possible. Area A of the electrodes is 20 × 50 mm. To supply a voltage for a precisely defined development time, an electronic high-voltage switch has been built. This device supplies voltages up to ±1000 V and times from 30 μs to 99 s with an accuracy of about 1 μs.

The circuit diagram for current measurements with this cell is depicted in Fig. 6. With this setup we do not directly measure the current $I(t)$, but rather the charge $Q(t)$. A capacitor C_M is switched in series to the cell with a high-

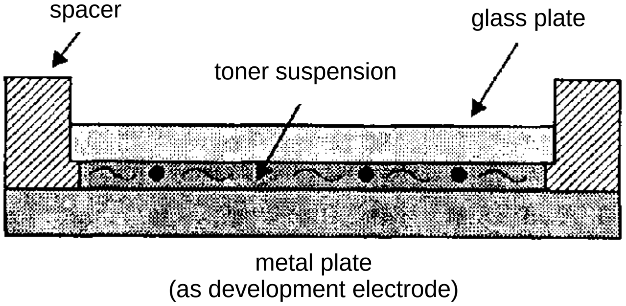

Figure 5. Sketch of the closed cell used for LID measurements.

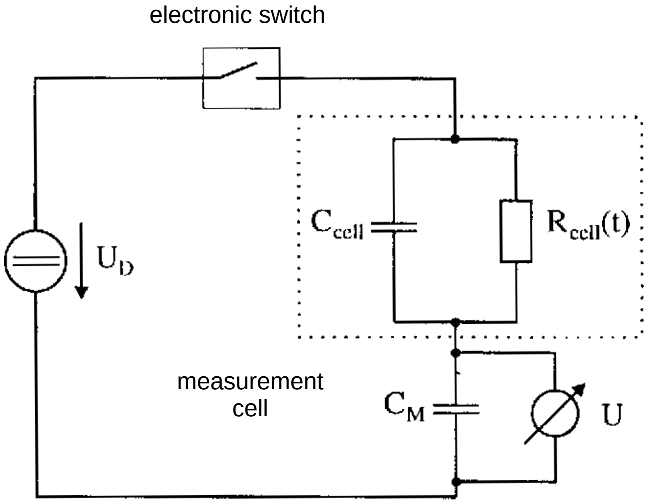

Figure 6. Circuit diagram for the measurement of the current in the external circuit of the closed cell of Fig. 5. A high-impedance voltmeter measures the voltage over the capacitor C_M. This voltage is proportional to the integrated current.

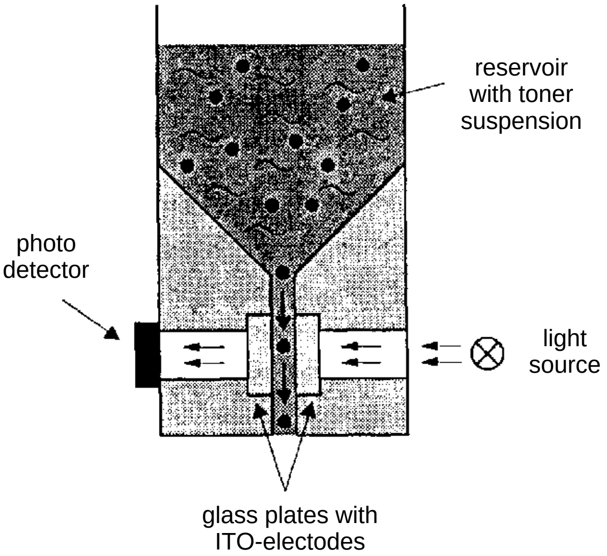

Figure 7. Schematic diagram for the cell with flowing toner to determine the mobility of the toner particles $\mu^{(T)}$.

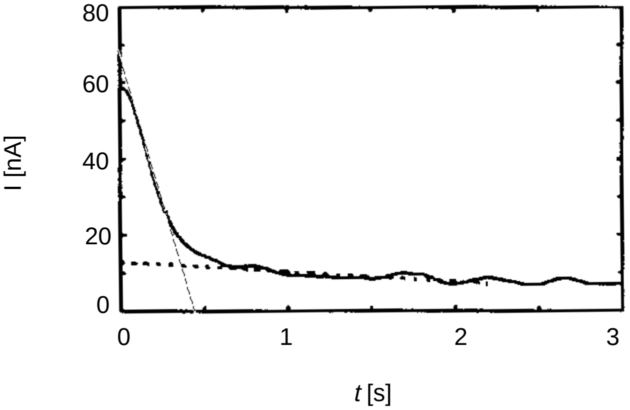

Figure 8. Measured current as a function of time for a cell as in Fig. 5. Parameters are U_D = 1000 V, d_D = 1.08 mm, k = 0.001%. The thin straight line is a fitting for the current for a short time and the dashed line is the part caused by the toner particles.

impedance voltmeter parallel to the capacitor C_M, which is much larger than the capacitance of the cell, so that the voltage drop on C_M can be neglected. The advantage of this method is that the high current flowing due to the charging of the cell capacitance results in only a voltage step, rather than a peak, as for normal current measurements with a resistor. The data of the high-impedance voltmeter is A/D converted and recorded on a PC. If the current $I(t)$ is needed, the obtained charge curves $Q(t)$ are smoothed by an interpolating spline and then numerically differentiated.

The cell for the measurement of the optical transmission density as a function of time for highly diluted toner suspensions is shown in Fig. 7. Two transparent electrodes with a distance of 215 μm are made of ITO-coated glass plates. Parallel light passes through the development region and falls on a photodetector. A continuous liquid flow is caused by the weight of the toner suspension in the reservoir above. Due to the small distance between the electrodes, the amount of liquid removed from the reservoir is rather small, so that the velocity of the liquid is approximately constant during an interval of 10 s.

Results

Toner Particle Mobility $\mu^{(T)}$**.** For the determination of $\mu^{(T)}$ we must fulfill the condition of negligible space charge (Eq. 10) in order to guarantee the validity of Eq. 27. For this we need the value for the charge density ρ_0 in the liquid toner. But, as ρ_0 is determined by the method described above, which needs a value for $\mu^{(T)}$, an iterative method is introduced. Additionally we must consider the flow of the liquid toner through the development region, so that all of the toner parameters are required in order to use the simulation program SimLID to verify that Eq. 27 holds.

Using the toner parameters obtained later and varying them in the range from half to double the normal value confirms with SimLID the validity of Eq. 27.

For the determination of $\mu^{(T)}$ we used the following parameters: applied voltage U_D = 50 V, distance between the electrodes d_D = 215 μm, toner concentration of k = 0.001% solids, and average flow velocity of 0.08 m/s. With Eq. 27 we achieve $\mu^{(T)} = 7.5 \times 10^{-10}$ m²/Vs. Due to slightly changing measurement results and a possible error for d_D, the range for $\mu^{(T)}$ is ±15%.

Determination of ρ_0, φ, **and** λ**.** The following conditions have been used to determine the missing three parameters with the closed cell: applied voltage U_D = 1000 V, distance between the electrodes d_D = 1.08 mm, and toner concentration of k = 0.001%.

Figure 8 shows a typical curve for the current $I(t)$. Two straight lines have been fitted in order to determine $\tau^{(XC)}$, $I_0^{(TXC)}$, and $I_0^{(T)}$. Because of the nonzero current for long times t, it is rather difficult to find the "right" fitting of the line for the current caused by the toner particles. If we had determined $\mu^{(T)}$ from this straight line, a large error would have been unavoidable. But, because $\mu^{(T)}$ is already known, we can calculate $\tau^{(T)}$, thus severely enhancing the accuracy of the fitting.

Repetitive measurements of current curves show only moderate reproducibility, even though great care has been taken to ensure constant conditions. There are several reasons for these deviations. One of them is the high dilution of the toner suspension, so that the current is very low and noise disturbs the measurements. Additionally, the

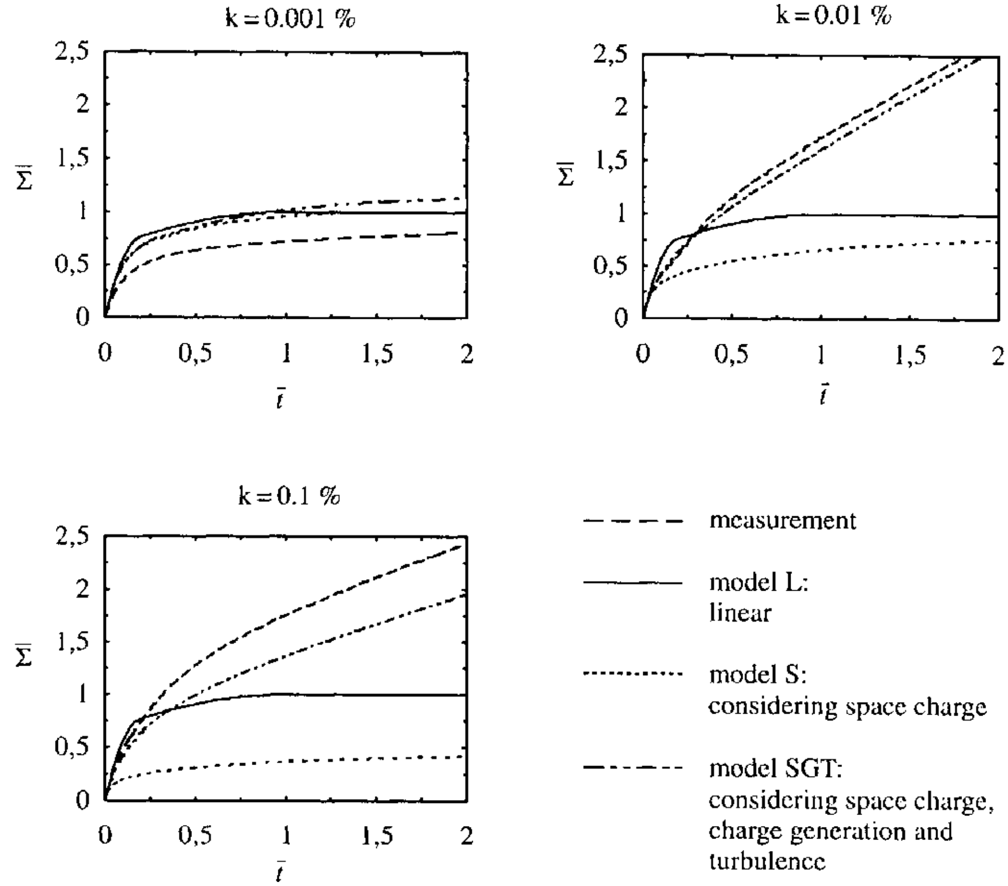

Figure 9. Normalized charge $\bar{\Sigma}$ in the external circuit of a closed cell as a function of normalized time $\bar{t}$ for U_D = 100 V. In addition to the measured curve, the results of the calculations for three different models are depicted for each of the three toner concentrations (k = 0.001, 0.01, and 0.1%).

discussed complexities have some influence, even though this influence is held low by the dilution.

Averaging more than nine measurements leads to the following results for a toner suspension with 0.001% solids:

- λ = 5.5 (±25%)
- φ = 0.73 (±50%)
- ρ_0 = 0.0113 C/m^3 (±50%).

The relatively large possible errors are for the reasons discussed above and due to the fact that λ depends on $\mu^{(T)}$, which also has a possible error, and φ and ρ_0 depend on λ. With other distances d_D (e.g., d_D = 0.55 mm) or slightly higher concentrations (e.g., 0.002% solids) similar results were achieved.

With the value for ρ_0 we can check if space charge according to Eq. 10 is negligible. With $\varepsilon_D = 2$ for the toner suspension, the right-hand side of Eq. 10 equals 0.030 C/m^3. Thus we are not on the safe side, but the simulation program SimLID proved that under the specified conditions the influence of space charge on the current $I(t)$ is less than 5%. Finally, λ = 5.5 verifies the assumption made previously, that excess and counter ions have a higher mobility than the toner particles.

Space-Charge Range. Now, with the determined toner parameters and SimLID, we can calculate the LID process also for nonnegligible space charge and compare calculated and measured data. Here we deal with the transported charge. The number of deposited toner particles is treated in a following section.

Figure 9 shows the transported charge in the cell of Fig. 5 for different toner concentrations as a function of time for d_D = 1.08 mm and U_D = 100 V. Corresponding results for U_D = 1000 V are depicted in Fig. 10. The transported charge is normalized to the charge* for the particles of one polarity being initially present in the development region:

$$\bar{\Sigma} = \frac{\Sigma}{d_D \rho_0}. \tag{28}$$

The value for the charge density ρ_0 = 0.0113 C/m^3 for a concentration of k = 0.001% is linearly extrapolated for higher concentrations (e.g., ρ_0 = 1.13 C/m^3 for a concentration of k = 0.1%). Time t is normalized to the time $\tau^{(T)}$, which a toner particle in the linear model needs to migrate through the development region:

$$\bar{t} = \frac{t}{\tau^{(T)}} \text{ with } \tau^{(T)} = \frac{(d_D)^2}{\mu^{(T)} U_D}. \tag{29}$$

For every concentration, four different curves are shown:

1. A measured curve representing a typical result (dashed line). Deviations of other measured curves under similar conditions are about 5 to 10%, or higher especially for a low concentration k. The voltage jump that occurs through the charging of the capacity of the cell has been subtracted.
2. Linear model (Model L, unbroken line). Note that the curve for the charge $\bar{\Sigma}(t)$ is not a straight line, but rather a parabola, because $\bar{\Sigma}(t)$ results from the integration of the current $I(t)$ (Eq. 18).
3. Space-charge model (Model S, finely dashed line). The calculation has been performed with the simulation program SimLID.

---

* For convenience we will talk of "charge" even though the quantity $\rho_0 d_D$ has the units of a surface charge.

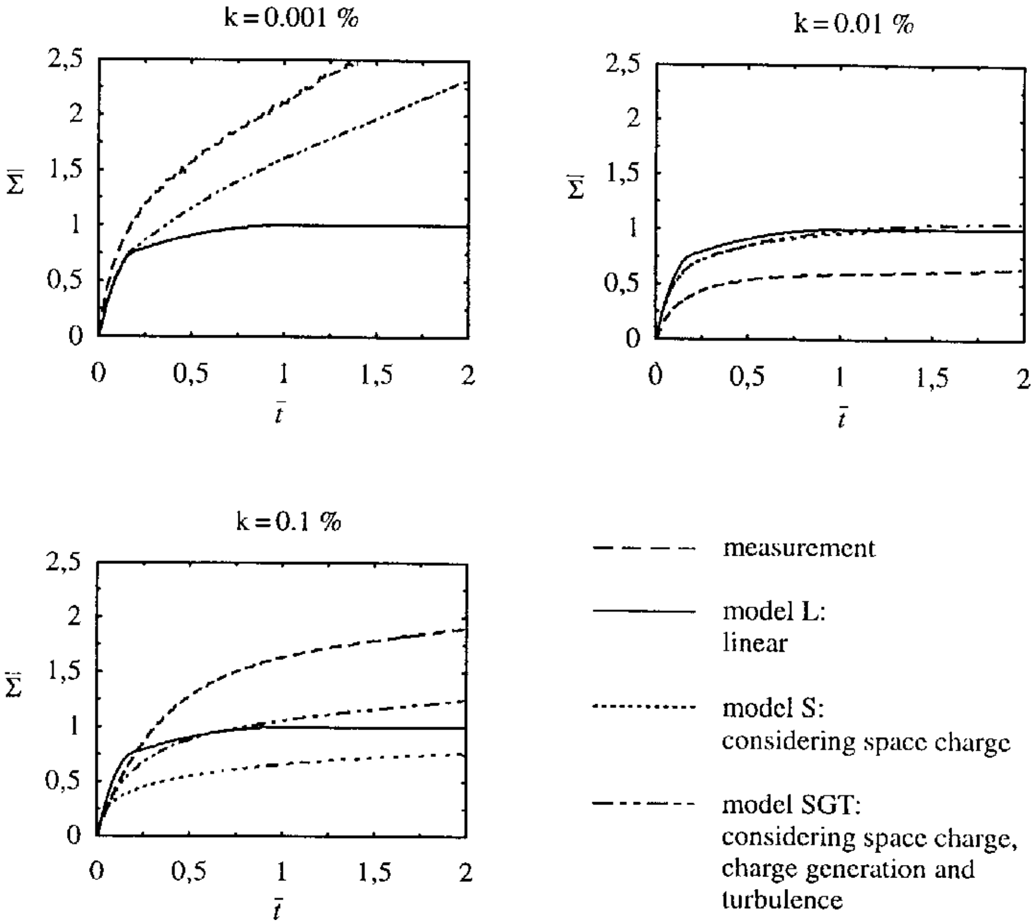

Figure 10. As in Fig. 9, but with U_D = 1000 V. For k = 0.001% the curves of the linear model (Model L) and the space charge model (Model S) match because here space charges may be neglected.

TABLE I. Values for the Charge Generation Constant g (in s^{-1}) and the "Diffusion" Constant $\tilde{D}_{turb}$ (in m^2/s) of the Extended Space-Charge Model (Model SGT) in Figs. 9 and 10

	k = 0.001%	k = 0.001%	k = 0.1%
U_D = 100 V	g = 0.005; $\tilde{D}_{turb}$ = 0	g = 0.07; $\tilde{D}_{turb}$ = 10^{-7}	g = 0.04; $\tilde{D}_{turb}$ = 10^{-7}
U_D = 1000 V	g = 0.5; $\tilde{D}_{turb}$ = 0	g = 0.02; $\tilde{D}_{turb}$ = 0	g = 0.1; $\tilde{D}_{turb}$ = 10^{-6}

4. Extended space charge model (Model SGT). In addition to space-charge effects, charge generation, as well as turbulence, has been considered. The calculations have been performed with the simulation program SimLID and the discussed methods for the description of charge generation and turbulence effects have been used. Values for the charge generation constant g and the "diffusion" constant $\tilde{D}_{turb}$ have been found iteratively with the premise for a best fit between measured and calculated curve. The obtained values are summarized in Table I.

A first look at the measured curves reveals that in most cases $\bar{\Sigma}(t)$ rises above 1. This means that the amount of charge that has been measured is higher than the amount initially present in the development region. This rise is due to charge generation, which obviously is not negligible here. Consequently the approximation of the measured curves with Model L and Model S is rather poor, except for high electric fields, low concentration, and relatively short development time, where generation effects are not yet important. The extended space-charge model (Model SGT) shows better results, even though obvious deviations remain in some cases.

Discussion

Deposited Charge. A closer investigation shows that the shape of every single measured curve is in good agreement with the corresponding curve of the extended space-charge model (Model SGT). We were able to show that an error of less than about 5% can be obtained if the value for the space-charge density ρ_0 is changed for every individual curve within a range from half to double the normal value. Within this range the calculated curves in Figs. 9 and 10 remain approximately unchanged, as the normalized form $\left[\bar{\Sigma}(\bar{t})\right]$ is depicted and only the measured curves change according to the change in ρ_0.

This result might be due to a nonlinear dependence of the charge density ρ_0 of the concentration k of the toner suspension. To check this, pulse measuring techniques have been used. Such techniques were first described by

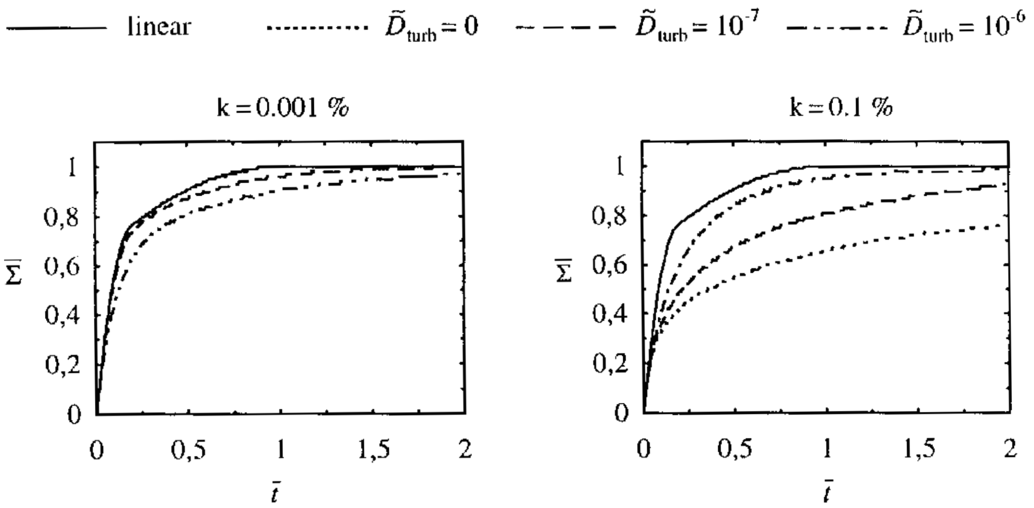

Figure 11. Normalized charge $\bar{\Sigma}$ in the external circuit of a closed cell as a function of normalized time $\bar{t}$ for U_D = 1000 V and differently strong turbulence. The strength of the turbulence is simulated by a diffusion constant $\tilde{D}_{turb}$ (in m²/s).

Watson and Sharbaugh.[30] This method measures the charge flow in an external circuit of a cell as in Fig. 5 for short development times. The reasonable assumption is made that, for short development times, space-charge and other disturbing effects (e.g., charge generation and turbulence) can be neglected. Thus the linear model according to Eq. 18 is valid, leading to a rather simple relationship for current and transported charge.

The measurements have been performed over a wide range of parameters. We find that the charge density ρ_0 is linearly related to the toner concentration k. This result is in agreement with observations of several other authors.[3,4,6,7,10] Thus, there must be a different reason for the observed deviations between the measured curves and our extended space-charge model. Our proposed explanation, which is rather complex, is based on a coupling effect between turbulence and space-charge influences.

Figure 11 shows the influence of turbulence (simulated by a diffusion constant $\tilde{D}_{turb}$) on the charge $\bar{\Sigma}(\bar{t})$ flown in the external circuit. All curves were calculated with the simulation program SimLID and U_D = 1000 V; and other parameters are as in Fig. 9. For the low toner concentration (k = 0.001%) the influence of space charge can be neglected, so that the curves for Model L and Model S ($\tilde{D}_{turb}$ = 0) match. Including turbulence leads to decreasing values for $\bar{\Sigma}(\bar{t})$ with increasing $\tilde{D}_{turb}$ ($\tilde{D}_{turb} = 10^{-7}, 10^{-6}$). For the high toner concentration (k = 0.1%) the curve for Model S ($\tilde{D}_{turb}$ = 0) is considerably below that for Model L. [Note that here the curve of the space charge model (Model S) does not exceed the curve for the linear model (Model L) as in Fig. 2, because here we look at the amount of charge flow in the external circuit of the cell rather than the amount of deposited charge of one particle type on the surface of the corresponding electrode.] With higher $\tilde{D}_{turb}$ the value for $\bar{\Sigma}(\bar{t})$ rises and reaches a maximum at about $\tilde{D}_{turb} = 10^{-6}$. A further increase of $\tilde{D}_{turb}$ leads to decreasing $\bar{\Sigma}(\bar{t})$ (not shown).

A qualitative explanation can be found with the help of Fig. 3 and the model, which has been described, for the temporary rise of the deposited charge with space-charge influence.

First, for the low toner concentration (k = 0.001%), we can neglect space charges and we have a situation similar to Fig. 3(b), the only difference being that the electric field is approximately constant over the complete development region. Turbulence, simulated by a diffusion coefficient $\tilde{D}_{turb}$, leads to an equalization of the particle distribution, so that the jump of the particle distribution is smoothed and less charge flows than with the undisturbed case.

Second, for the high toner concentration (k = 0.1%), we have a situation similar to Fig. 3(c), with depletion zones near the electrodes, which at the same time are zones of an increased electric field. After a short period of accelerated development, these zones slow down the development process because the electric field, and thus the migration speed in the center of the development region, is decreased. Now, with turbulences, particles are transported into the depletion zones, and they then move rather fast due to the local high electric field, so that an enhanced development compared with $\tilde{D}_{turb}$ = 0 is observed.

This gives so far no explanation for the deviation of the curves of the measurement and the extended space charge model (Model SGT) for k = 0.001% and U_D = 1000 V. The curve depicted in Fig. 10 for Model SGT has been calculated with $\tilde{D}_{turb}$ = 0. A value of $\tilde{D}_{turb}$ > 0 would further decrease the curve of Model SGT and therefore increase the deviation. We believe that the main reason for the deviation is an error in the determination of the space-charge density ρ_0 because of an excess current due to injection effects. This explanation is supported by the very high value for the charge generation constant g = 0.5 for this voltage and toner concentration. All other values for g are considerably smaller. Injection effects are probably the main reason for the seemingly high generation constant g. The occurrence of injection effects has been reported by other authors.[31,32] This effect, the injection of charged particles into a low concentration fluid, leads to a nonlinear field-dependent conductivity and is most pronounced at high field strength (U_D = 1000 V) and low toner concentration (k = 0.001%). For higher concentrations the amount of charge due to injection becomes small compared with the charge of the particles of the toner suspension.

An alternative method for the determination of the charge density ρ_0 of a toner suspension, which is commonly used,[8] is the integration of the total current flowing in the external circuit of the measurement cell. From Eq. 18 we derive $Q_{total} = Ad_2\rho_0$. This value actually is independent of space charge and turbulences, because, after a sufficient time, all of the charge of the liquid is deposited on the electrodes. However, it is not independent of charge generation effects. Commonly such effects are accounted for by subtracting the value of the current for a steady state after the end of the regular development process from the measured current. Measurements and simulations with the simulation program SimLID showed that the accuracy of

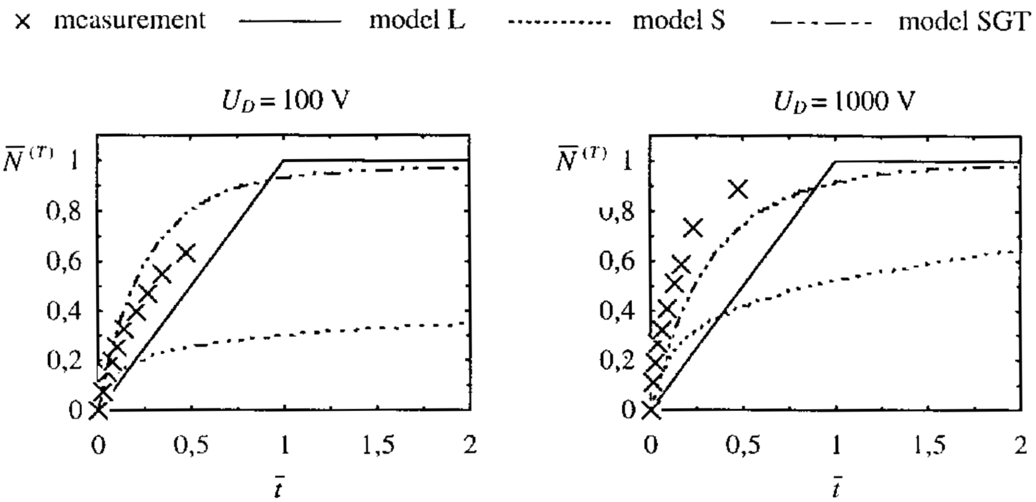

Figure 12. Normalized number of deposited toner particles $\overline{N}^{(T)}$ as a function of normalized time $\bar{t}$. In addition to the measured values, the results of the calculations for three different models are depicted.

this method with the investigated toner is typically lower than the method (described above) we used for the determination of ρ_0.

The only method left for an improved value for ρ_0 is an estimation that considers the curves of Figs. 9 and 10 as well as the discussion about injection effects. This and simulations with SimLID lead to $\rho_0 = 0.006$ to 0.008 C/m^3 for $k = 0.001\%$.

With this value for ρ_0 we can explain Figs. 9 and 10. First we look at Fig. 10, $U_D = 1000$ V. The "real" measured curve for $k = 0.001\%$ is due to the injection current considerably below the depicted one, so that there is an improved agreement with the extended space-charge model (Model SGT). For $k = 0.01\%$ a smaller value of ρ_0 leads to a measured curve above the depicted one, again leading to an improved agreement. The curve for the highest concentration ($k = 0.1\%$) rises with the new and lower ρ_0. Here we must consider that our description of turbulence by a diffusion constant $\tilde{D}_{turb}$ is only a simplified model for the complex effects of turbulences. Thus we cannot expect a high accuracy from this model. However, our Model SGT explains the fact that the measured curve $\overline{\Sigma}(\bar{t})$ is considerably higher than might be expected when only space charges are considered.

The explanations for $U_D = 100$ V (Fig. 9) are analogous to the discussion above for $U_D = 1000$ V. For $k = 0.001\%$ the lower value for ρ_0 leads to better agreement, while we have the same situation for higher concentrations ($k = 0.01$ and 0.1%) as for $U_D = 1000$ V and $k = 0.1\%$.

Altogether, considering the fact that the description of turbulence is roughly approximated by a diffusion constant $\tilde{D}_{turb}$, we have good agreement between the measurements and our extended space-charge model. The values for $\tilde{D}_{turb}$ given in Table I fit into the described model. For the low toner concentration ($k = 0.001\%$) we have $\tilde{D}_{turb} = 0$ for $U_D = 100$ and 1000 V, which agrees with the idea that turbulence effects are negligible at low toner concentrations. For higher concentrations we have a higher value for $\tilde{D}_{turb}$ for the high voltage ($U_D = 1000$ V), which is reasonable because we expect stronger turbulences for faster particle movement.

Deposited Toner Particles. So far we have considered the amount of charge flow in the external circuit of the measurement cell. For most applications another quantity, the amount of deposited toner per unit area $N^{(T)}$, is more relevant. Figure 12 shows $\overline{N}^{(T)}$ as a function of $\bar{t}$. Normalization here is just as before, for the charge Σ:

$$\overline{N}^{(T)} = \frac{N^{(T)}}{d_D n_0^{(T)}}. \qquad (30)$$

Analogous to Figs. 9 and 10, Fig. 12 shows four curves: measured values, Model L, Model S, and the extended space-charge model (Model SGT). All parameters are as with Figs. 9 and 10. The measured values were achieved by measuring the optical transmission density D_{TR} of the deposited toner particles on the transparent ITO electrode of the cell. According to Eq. 25, $N^{(T)}$, and thus $\overline{N}^{(T)}$ is proportional to D_{TR}. With this relation it is convenient to normalize D_{TR} to the value achieved for very long development time, when all toner particles have definitely been deposited on the electrode. Thus we do not need a value for $n_0^{(T)}$, verifying the assumption made above that four parameters (ρ_0, φ, $\mu^{(T)}$, λ) are sufficient for a complete characterization of the toner suspension. In Fig. 12, only values for $k = 0.1\%$ are shown, as the optical transmission density is too low for precise measurements for lower concentrations.

A first result (not shown here) is that the number of deposited particles shows only a very weak dependence on the charge generation constant g and ratio λ. It is obvious that here all measured values are above those of the linear model. This cannot be understood in terms of older models, whereas the extended space charge model (Model SGT), which considers the coupling between space charge and turbulence, explains this effect.

In addition to an acceleration of the development, the coupling of space charge and turbulence has a linearization effect: If we look at the measured values, it is obvious that a straight line is a good approximation for the values of $U_D = 100$ V and also for $U_D = 1000$ V if $\bar{t} < 0.25$ is taken. Thus, if nothing about the mobility of the toner particles $\mu^{(T)}$ is known, an interpretation of the measurements could be that a linear model (as described by Eq. 4) is a good approximation for the development process. However, as can be seen from Fig. 12, the value for $\mu^{(T)}$ determined by a straight line through the measured values deviates considerably from the true value indicated by the straight line of Model L.

This fact is a good explanation for the results of several previous authors, which state good agreement between their measured results and a linear model for LID,[†] that neglects space charge and other complexities. According to our understanding, the seemingly linear relationship is caused by the coupling between space charge and turbulence, so that in our opinion the pure linear approximation has two

---

[†] Note that the linear model in other papers typically refers to situations with a photoconductor, so that the number of deposited particles is described by an exponential function rather than by a straight line. However, this does not alter the results of our discussion.

major disadvantages: First, the toner parameters (especially $\mu^{(T)}$) do not agree with typical conditions for LID, and second, the "linearity" does not hold when the development process comes close to saturation.

Finally we want to mention briefly an effect reported by several previous authors, namely, the field dependence of the electrophoretic mobility of the toner particles $\mu^{(T)}$.[33–35] Even though we must still perform further investigations, our first results showed only a very weak relation between $\mu^{(T)}$ and the electric field strength. To our knowledge, the previous authors did not consider space charge and other complexities, so that the measured values for $\mu^{(T)}$ might result from effects other than a field dependence of $\mu^{(T)}$.

Summary and Conclusions

The process of liquid immersion development has been thoroughly investigated, theoretically as well as experimentally. Even though the ultimate goal, a complete and accurate model for the description of the LID process, is still a long way off, we believe that this study is a step towards this goal. The most important results are now briefly summarized:

- A simple theoretical analysis reveals that for typical conditions of LID the linear relation does not hold because of space-charge effects. We present a formula that defines an estimation for conditions under which the linear model is valid.
- A theoretical investigation of the LID process with consideration of space charge leads to the surprising result that space charge causes an acceleration of the development (number of deposited particles) compared with the linear model for a short time.
- Methods for the measurement of parameters of toner suspensions are presented. It is important to use highly diluted suspensions in order to minimize the influence of space charge and other complexities.
- For higher toner concentrations turbulence plays an important role. For a first approximation, we propose to describe the influence of turbulences by a diffusion constant.
- A rather complex model for the LID process that we present includes space-charge, charge generation, and turbulence effects. This model achieves good quantitative agreement with the measurements for low concentrations and a good qualitative and fair quantitative agreement for medium and high concentrations.
- The coupling of space charge and turbulence effects for high concentrations leads to a considerably more accelerated development (larger number of deposited particles) than that predicted by a linear or space-charge model. Additionally the coupling leads to an approximately linear relationship as long as development does reach saturation.

An improvement of the model can be expected when our rather simple first-order approximations for charge generation and turbulence are replaced by more accurate descriptions. Measurements of the toner parameters may be improved by using electrodes with thin insulating coatings in order to avoid injection effects.[13,32]

Acknowledgment. The authors wish to thank B. Hill for his helpful suggestions and enlightening discussions. Part of this work was sponsored by the "Deutsche Forschungsgemeinschaft" (DFG), Bonn, Bad Godesberg.

References

1. K. A. Metcalfe, *J. Sci. Instr.* **32**: 74 (1955).
2. M. Schleusener, *J. Signal AM.* **5***:* 39 (1977); *ibid.* **5**: 93 (1977).
3. J. A. Dahlquist and I. Brodie, *J. Appl. Phys.* **40**: 3020 (1969).
4. H. M. Stark and R. S. Menchel, *J. Appl. Phys.* **41**: 2905 (1970).
5. R. M. Schaffert, in *Electrophotography,* 2nd Ed., Focal Press, London, New York, 1975.
6. R. Kohler, D. Giglberger, and F. Bestenreiner, *Photogr. Sci. Eng.* **22**: 218 (1978).
7. J. Halfdanarson and K. Hauffe, *Photogr. Sci. Eng.* **23**: 27 (1979).
8. V. Novotny and M. L. Hair, *J. Colloid Interface Sci.* **71**: 273 (1979).
9. H. Murray, *IEEE Trans. Ind. Appl.* **IA-23**: 831 (1987).
10. T. G. Davis, G. A. Gibson, R. H. Luebbe, and K. Yu, *Proceedings of SPSE's 5th International Congress on Advances in Non-Impact Printing Technologies*, 1989, p. 417.
11. S. Kuramoto and K. Tsubuko, *Proceedings of SPSE's 6th International Congress on Advances in Non-Impact Printing Technologies*, 1990, p. 557.
12. L. B. Schein, *Electrophotography and Development Physics,* 2nd ed., Springer, New York, 1992, pp. 203–244.
13. L. B. Schein, G. P. Gee, M. H. Lee, and C. I. Dodds, *J. Imaging Sci. Technol.* **38**: 409 (1994).
14. M. Schleusener, *Wiss. Zeitschr. TH Magdeburg* **21**: 655 (1977).
15. M. Croucher, S. Drappel, J. Duff, G. Hamer, K. Lok, and R. Wong, *Phtogr. Sci. Eng.* **28**: 119 (1984).
16. G. Bartscher, J. Breithaupt, and B. Hill, *Proceedings of IS&T's 11th International Congress on Advances in Non-Impact Printing Technologies*, 1995, p. 529.
17. G. Bartscher, J. Breithaupt, and B. Hill, *J. Imaging Sci. Technol.,* **40**:14 (1996).
18. K. A. Metcalfe and R. J. Wright, *J. Sci. Instr.* **33**: 194 (1956).
19. T. Kurita, *Denshi Shashin (Electrophotography)* **3**: 26 (1961).
20. P. E. Castro and W. C. Lu, *Photogr. Sci. Eng.* **22**: 3 (1978).
21. C. C. Yang and G. C. Hartmann, *IEEE Trans. Electron Devices,* **23**: 308 (1976).
22. R. B. Crofoot and Y. C. Cheng, *J. Appl. Phys.* **50**: 6583 (1979).
23. I. Chen, *J. Imaging Sci. Technol.* **32**: 201 (1988).
24. R. W. Hockney and J. W. Eastwood, *Computer Simulation Using Particles,* Adam Hilger, 1989.
25. G. Bartscher, *Investigation of a New Electrophoretic Printing Process,* Dissertation, Aachen University of Technology, Germany, 1995 (in German).
26. T. Van der Ven, *Colloidal Hydrodynamics,* Academic Press, London, 1989.
27. R. Stechemesser, *Photogr. Sci. Eng.* **26**: 27 (1982).
28. I. Chen, *J. Appl. Phys.* **45**: 4852 (1974).
29. B. E. Bayer, *J. Opt. Soc. Am.* **54**: 1485 (1964).
30. P. K. Watson and A. H. Sharbaugh, *Rev. Sci. Instr.* **35**: 1310 (1964).
31. G. Molinari and A. Vivani, *J. Electrostatics,* **7**: 21 (1979)); *ibid.* **7**: 27 (1979).
32. V. Novotny, *J. Electrochem. Soc.* **133**: 1629 (1986).
33. P. H. Wiersma, A. L. Loeb, and J. Th. G. Overbeek, *J. Colloid Interface Sci.* **22**: 78 (1966).
34. S. Stotz, *J. Colloid Interface Sci.* **65**: 118 (1978).
35. Y. Niv, Y. Adam, and Y. Krumberg, *Proceedings of SPSE 3rd International Congress on Advances in Non-Impact Printing Technologies, Advance Printing of Paper Summaries*, SPSE, 1986, p. 57.